Final report for Hypoxic-directed Magnetic Resonance-guided Focused Ultrasound Therapy:

The initial 8 months of our project were devoted to optimizing a co-registration system for PET/MRI imaging allowing us to identify and target hypoxic regions in solid tumors. The aim of this work was to develop and test a preclinical noninvasive ablation system to selectively ablate hypoxic tumor in small animal studies. The rationale was and still is to develop a method to destroy regions of the tumor that are typically resistant to standard treatments and reduce the time required for typical whole tumor ablation. The system is composed of a Micro positron emission tomography (PET), 7T magnetic resonance imaging (MRI), and MRI-compatible focused ultrasound applicator. To identify hypoxic regions, 18Ffluoromisonidazole (18F-miso) radioactive tracer was administered intravenously via the tail veins of mice. Tracer uptake in the tumors was quantitatively measured by PET imaging and the tumor hypoxic regions were delineated based on a threshold tumor/muscle activity ratio. The tumor hypoxic regions were targeted for ablation by overlapping the PET hypoxic regions on the high resolution multi-slice MR anatomical images. A customized MRI-compatible spherically-focused ultrasound applicator for small animals was used to ablate the PET-validated hypoxic targets with the guidance of real-time MR temperature imaging; this work was submitted for publication and is now being prepared for resubmission.

In addition, the final 10 months of the project, including a 6 month no cost extension, have focused on a novel approach discovered in our lab during the initial work based on high-frequency ultrasound mapping of tumor vascular hypoxia as a targeting modality for focused ultrasound ablation to complement ionizing radiotherapy (please see figures 1-3 below). This project was presented at the 3rd FUSF meeting in fall of 2012 and we are continuing to develop the method as a new and better alternative to identify and destroy hypoxia in solid tumors or other diseased states using HIFU. PI Griffin was invited to speak at the AAPM meeting August 6, 2015 about this approach and also reported on the work at the 2012 Radiation Research annual meeting and the 2013 Society for Thermal Medicine meetings in invited presenations as well. Our discovery of this new approach and the exciting possibilities that it presents were the major reason for requesting an extension of the original funding period. The current state of that work and rationale is that a method to identify and destroy regions of vascular hypoxia in solid tumors with HIFU could reduce treatment times and greatly improve overall tumor control. Based on the idea that markers for hypoxia, nitroimidazole's, produce detectable cell surface antigens on radiobiological hypoxic cells, a full time graduate student in our laboratory has begun an investigation of targeted microbubbles for detecting endothelial/blood adjacent cell hypoxia. We surmise that antibody-targeted high-frequency ultrasound mapping of endothelial/blood adjacent hypoxia may be an improved approach for focused ultrasound ablation of these areas to complement radiation or chemotherapy. As alluded to above, our initial work on PET/MRI-guided focused ultrasound (PET/MRgFUS) with 18F- misonidazole for detection of regional tumor hypoxia and selective ablation of these areas proved that a rationale for combined HIFU and radiotherapy exists. However, this approach is inefficient in spatial resolution of tumor hypoxia and cumbersome for clinical translation (very expensive and difficult to schedule the multimodality imaging required). Our modified approach of detecting and targeting regions of vascular hypoxia using ultrasound detection and subsequent MRg FUS ablation has led to two follow on funding requests to the NIH- one is an F31 training award for Nathan Koonce, PhD candidate, and one is a renewal of PI Griffin's current R01 funding on the physiology of thermal therapy. Ultimately we aim to incorporate the imaging and targeting of hypoxia using both diagnostic and MRgFUS into advanced combined regimen treatment with radiotherapy and targeted drug delivery to these areas as illustrated in figure 3. The pilot funding from the FUSF was instrumental in moving us closer to that goal on many levels.

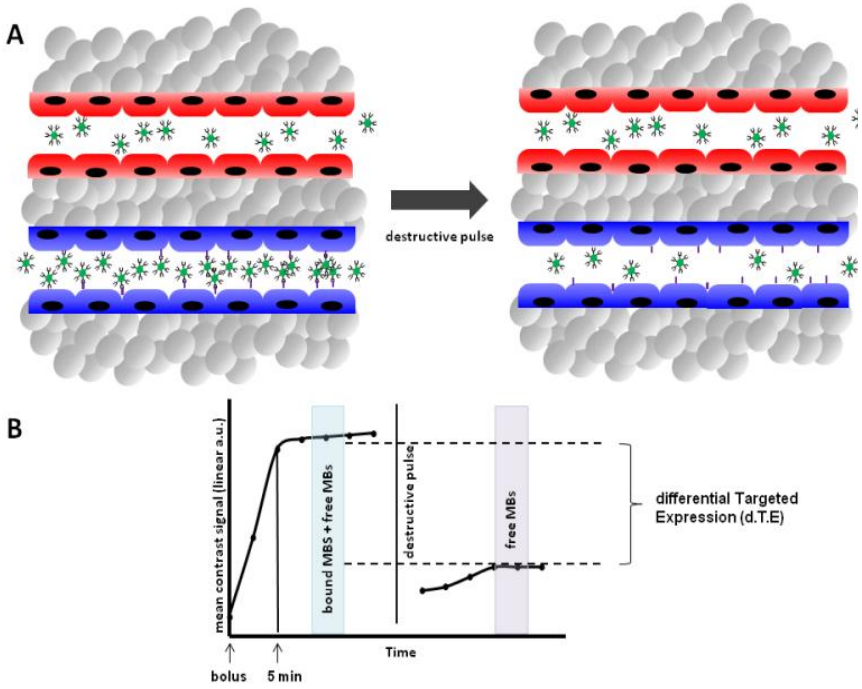

Figure 1. Schematic of anti-pimonidazole targeted microbubbles with US imaging for detection of vascular hypoxia. A) Illustrates the differential distribution of $MB_{pimonidazole}$ in well oxygenated tumor endothelium **(red, top)** compared to hypoxic tumor endothelium **(blue, bottom)**.
B) Representative quantification graphic of $MB_{pimonidazole}$ where the binding occurs over a 5 minute window after IV injection followed by a data collection period of contrast signal for ~20sec burst bound and free $MB_{pimonidazole}$, reperfusion window and then comparison is made from the steady state prior to microbubble burst and following burst. This differential targeted expression (d.T.E.) represents the relative amount of bound bubbles to their antigen or indirectly the location and amount of vascular hypoxia within the tumor.

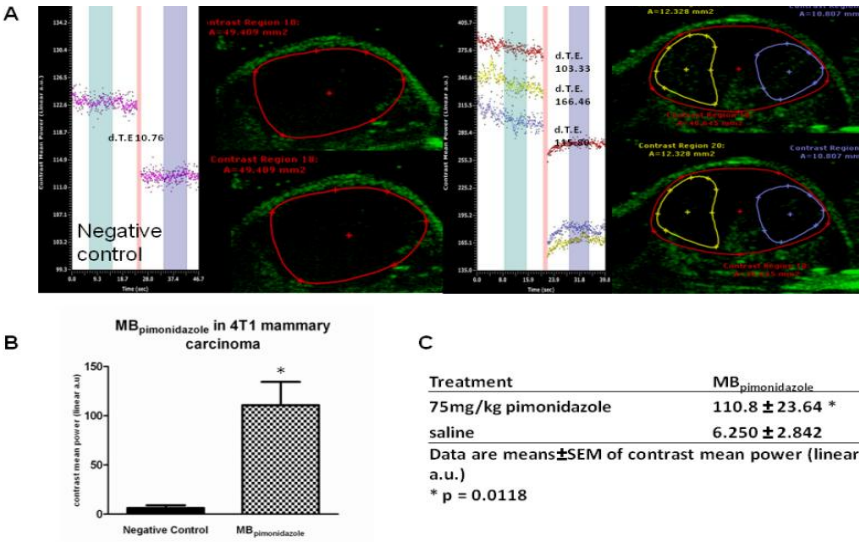

C

Treatment	$MB_{pimonidazole}$
75mg/kg pimonidazole	110.8 ± 23.64 *
saline	6.250 ± 2.842

Data are means±SEM of contrast mean power (linear a.u.)
* p = 0.0118

Figure 2. Quantitative analysis of vessel hypoxia by anti-pimonidazole targeted microbbubles in control and pimonidazole-injected tumor bearing mice. A) 4T1 tumor bearing Balb/c mice were injected with 75mg/kg pimonidazole **(right)** or saline **(left)** 2hr prior to injection with anti-pimonidazole targeted microbbubles, $MB_{PIMONIDAZOLE}$, for analysis of tumor vessel hypoxia. Top images are prior to destructive pulse of microbubbles and bottom images are following microbubble burst.
B) Quantified data from images in panel A show the specificity of $MB_{PIMONIDAZOLE}$ when animals are injected with pimonidazole in comparison to negative controls (saline treated), n = 3. **C)** Table form of quantified data showing a statistically significant 17-fold difference between microbubble targeting in control and pimonidazole injected mice, p = 0.0118.

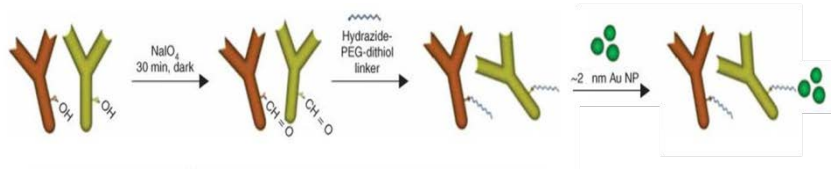

Figure 3. Anti-pimonidazole antibody linking strategy to DNA-linked gold nanoparticles. Addition of a PEG-dithiol linker to the Fc portion of the antibody allows for conjugation to DNA-linked gold nanoparticles (green), while maintaining an open Fab antibody fragment for targeting. The delivered particles could also be chemotherapy coated to improve chemoradiation response of hypoxic vasculature and tissue regions.